Journal of Catalysis **187,** 348–357 (1999)
Article ID jcat.1999.2623, available online at http://www.idealibrary.com on IDEAL®

Catalytic Reactions of Mixtures of Carbon Dioxide, Ethene, and Hydrogen on Cobalt Surfaces

M. Voß, G. Fröhlich, D. Borgmann,[1] and G. Wedler

Institute of Physical and Theoretical Chemistry, University of Erlangen-Nürnberg, Egerlandstr. 3, D-91058 Erlangen, Germany

Received February 16, 1999; revised June 29, 1999; accepted June 29, 1999

Using a plug-flow and a batch reactor the hydrogenation of mixtures of carbon dioxide and ethene over unsupported cobalt has been studied. The results show that the hydrogenation of carbon dioxide is totally blocked as long as ethene is present in the gas phase. In contrast carbon dioxide does not at all influence the hydrogenation of ethene, which leads to a complex mixture of hydrocarbons. This reaction can be explained as a copolymerisation proceeding via two different monomers (C_1 and C_2 fragments). The observed oscillatory molar product distribution in dependence on the number of C atoms can exactly be described by means of a numerical model.

Key Words: **cobalt; carbon dioxide; ethene; hydrogen; plug-flow reactor; batch reactor; Auger electron spectroscopy.**

1. INTRODUCTION

For several decades the Fischer–Tropsch synthesis on group VIII metals has been an intensely studied field in catalysis research and has been well described in the literature (1–6). The mechanism of CO hydrogenation on various Co catalysts plays a dominant role. Product distribution and paraffin/olefin ratios over polycrystalline Co foils have been measured by Kuipers *et al.* (7, 8). Bartholomew *et al.* (9) have studied the adsorption of CO on alumina supported cobalt catalysts. They report that at 523 K dissociation of CO leads to the deposition of carbon which can be hydrogenated to methane. These results correlate very well with our own measurements (10).

As compared with the hydrogenation of CO there are relatively few publications on the hydrogenation of CO_2. Reaction rates, product distributions, activities, and selectivities were determined on silica supported Co, Fe, and Ru catalysts (11), on polycrystalline Rh foils (12), and on alumina supported Rh and Ru catalysts (13, 14), as well as on silica and titania supported Rh (14). The high activity of the supported Rh catalysts was attributed to a strong metal-support interaction (SMSI effect). This effect could not be confirmed in the case of CO (15) and CO_2 (10) hydrogenation on Co/Al_2O_3, Co/SiO_2, and Co/TiO_2. Kinetics and the mechanism of the hydrogenation of CO_2 on silica supported Ni (and other group VIII metals) are still controversely discussed (16).

The present paper is part of a detailed model study of the hydrogenation of carbon dioxide over pure metallic cobalt catalysts and cobalt catalysts supported on Al_2O_3, SiO_2, and TiO_2. The study comprises the characterisation of the catalysts by means of various analytical methods (10), their activation and deactivation (17, 18), and the investigation of the reaction kinetics, as well as of the reaction mechanism (19).

Since the addition of carbon monoxide to the CO_2/H_2 feed led to interesting results concerning the activation and deactivation of the catalysts (20) the question concerning the action of other additives arose. It is well known from the literature (e.g., 21, 22) that ethene is able to act as a chain initiator and to influence both yield and selectivity of the hydrogenation of carbon monoxide (Fischer–Tropsch reactions). Thus it seemed to be worth investigating also the hydrogenation of carbon dioxide–ethene mixtures.

2. METHODS

In the course of the studies two types of apparatuses have been used which differ not only in the type of the reactor (plug-flow reactor and batch reactor) but also in the whole experimental equipment. They shall be separately presented. The catalyst used, however, was in all kinds of experiments a cobalt foil (Goodfellow), 0.05 mm thick and of purity 99.9%.

2.1. Plug-Flow Reactor

The plug-flow apparatus comprises a gas supplying system, a plug-flow reactor equipped with a programmable heating device, and a gas analysing system. The gas supplying system consists of a gas handling system which allows further purification of the high purity gases introduced from gas flasks, gas dosing by means of flow controllers (Brooks, Bronkhorst Hi-Tec), and gas mixing. The gas leaving the reactor can be dosed into a gas chromatograph (Carlo Erba, VEGA Series GC 6000) supplied with a Carbowax–Porasil column and a flame ionisation detector (for hydrocarbons)

[1] To whom correspondence should be addressed.

0021-9517/99 $30.00

as well as a Porapack QS column and a thermal conductivity detector (for carbon monoxide and carbon dioxide). Details of this apparatus have been published elsewhere (18).

The cobalt foil was cut into 7 mm × 1 mm × 0.05 mm pieces. Twenty-five pieces were introduced into the reactor. The catalyst was activated by at least 10 reduction and oxidation steps (15 ml_N/min H_2, 873 K, 10 h; 15 ml_N/min 0.1% O_2 in N_2, 823 K, 30 min) until its activity concerning the hydrogenation of carbon dioxide was constant. BET measurements showed that the surface of the activated cobalt foils exceeds the geometric surface area by a factor of 400. Further details concerning activation and deactivation of the catalyst have been reported elsewhere (18).

Measurements with the plug-flow reactor were carried out in the temperature range 433 K $\leq T \leq$ 533 K, since at lower temperatures the activation of the catalyst by the feed was too slow and at higher temperatures the deactivation by deposition of carbon was too fast.

2.2. Batch Reactor

The other apparatus is equipped with a continuously stirred batch reactor ($V = 275$ ml), a gas chromatograph (Carlo Erba, MEGA Series HRGC 5300), an ultrahigh vacuum (UHV) chamber with an Auger electron spectrometer (AES), and facilities for cleaning or preparing the cobalt foil, as well as a mass spectrometer in order to take thermal desorption spectra. A differentially pumped ultrahigh vacuum lock system connects the reactor and UHV chamber. The catalyst is fixed in a cut-out of a transfer rod and is heated by passing an electrical current through the cobalt foil. It can be transferred from the reactor into the UHV chamber and back by means of the transfer rod within a few minutes. Columns and detectors of the gas chromatograph are equal to those used in the plug-flow apparatus. Details of the whole device have been published in preceding papers (20, 23).

The cleaning procedure of a new foil started with repeated heating up to 1273 K, sputtering with neon ions ($I_{Ne} = 2.5\ \mu$A, $E_{Ne} = 750$ eV at 573 K) followed by reduction in 1 bar H_2. Between the different experiments both sides of the foil were sputtered with neon ions for 15 min. Oxidation in 100 mbar O_2 at 873 K for 30 min and reduction in 1000 mbar H_2 at 873 K for 12 h completed the procedure.

Auger electron spectroscopy has been used to control the cleaning process as well as to analyse the composition of the catalyst surface during the activation and the catalytic reaction.

3. RESULTS AND DISCUSSION

3.1. Hydrogenation of Carbon Dioxide–Ethene Mixtures in the Plug-Flow Reactor

The first question that should be answered is whether the presence of ethene influences the hydrogenation of carbon dioxide and vice versa. The use of a plug-flow reactor has proven to be the best way to answer this general question.

3.1.1. Influence of admission of ethene on the hydrogenation of carbon dioxide. Figure 1 refers to the hydrogenation of carbon dioxide on cobalt foils at $T = 493$ K. The feed consisted of 800 mbar hydrogen and 200 mbar carbon dioxide. The volumetric flow rate dV/dt was 60 ml_N/min. The turnover frequency of the product gases (carbon monoxide, methane, and ethane) is plotted in logarithmic scale against the time on stream.

Since the surface of the cobalt foils had been oxidised before the start of the experiment there is an induction period at the beginning, in which the surface is reduced. Steady-state conditions are achieved after about 60 min. Then the composition of the product gas is 54% CH_4, 40% CO, and 6% C_2H_6. Under these conditions the conversion of carbon dioxide amounts to less than 2%.

At $t = 150$ min 16 mbar ethene were admitted to the feed. This results in a drastic change of the composition of the product stream. The turnover frequencies of methane and ethane increase by a factor of 6 and 450, respectively. That of carbon monoxide decreases by 25%. The conversion of carbon dioxide decreases and that of ethene amounts to >95%. In addition significant amounts of both linear and branched alkanes and alkenes (up to C_7) are detected. The concentration of the saturated hydrocarbons exceeds that of the corresponding unsaturated hydrocarbons by one order of magnitude. The latter are reactive intermediates as will be shown later on.

This experiment indicates that the reaction is dominated by the hydrogenation of the admitted ethene and points to a hindrance of the hydrogenation of the carbon dioxide by the admitted ethene.

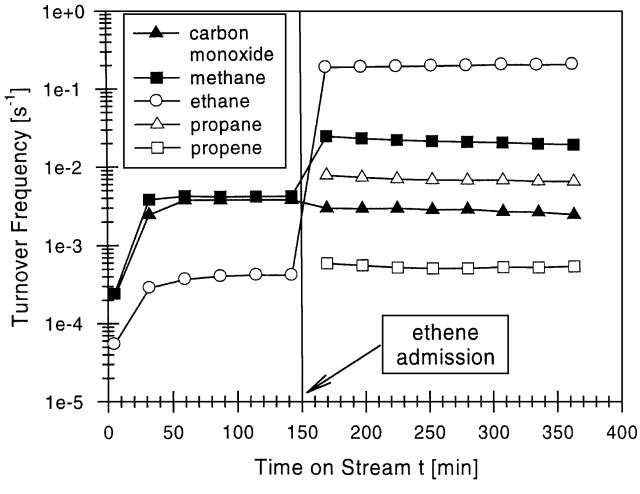

FIG. 1. Hydrogenation of carbon dioxide on cobalt foils in a plug-flow reactor at $T = 493$ K. At $t = 150$ min ethene was admitted to the feed.

3.1.2. Influence of the partial pressures of carbon dioxide and hydrogen on the selectivity of the hydrogenation of ethene. These experiments were performed at 433 K. Since the partial pressure of one of the components of the feed was changed in the course of the experiments, helium was admitted to adjust the total pressure always to 1000 mbar. The volumetric flow rate was again 60 ml_N/min.

In the first case the partial pressures of the feed were $p(H_2) = 800$ mbar, $p(C_2H_4) = 16$ mbar, $p(CO_2) =$ variable. Figure 2a shows the selectivity of the hydrogenation of ethene in logarithmic scale at varying carbon dioxide pressures. There is clear evidence that carbon dioxide does not influence the selectivity observed with the hydrogenation of pure ethene ($p(CO_2) = 0$ mbar), even when the partial pressure of CO_2 exceeds that of ethene by a factor of 12. The same holds when instead of the selectivity the yield is considered. The reaction is dominated by the direct hydrogenation to ethane (selectivity 95%; note that the logarithmic scale is enlarged in the upper part of Fig. 2a). However, methane, propane, and propene, as well as *n*-butane and 1-butene are formed too. It is interesting to note that under the given conditions the hydrocarbons with an even number of C atoms exhibit a higher selectivity than those with an odd number of carbon atoms. This observation will be picked up later in this paper.

In the second case the influence of the hydrogen pressure on the selectivity of the hydrogenation of ethene was studied. The partial pressures were $p(CO_2) = 200$ mbar, $p(C_2H_4) = 16$ mbar, $p(H_2) =$ variable. Figure 2b shows the result. An increase in hydrogen pressure leads to an increase of the direct hydrogenation of ethene. Simultaneously the probability of chain growth diminishes.

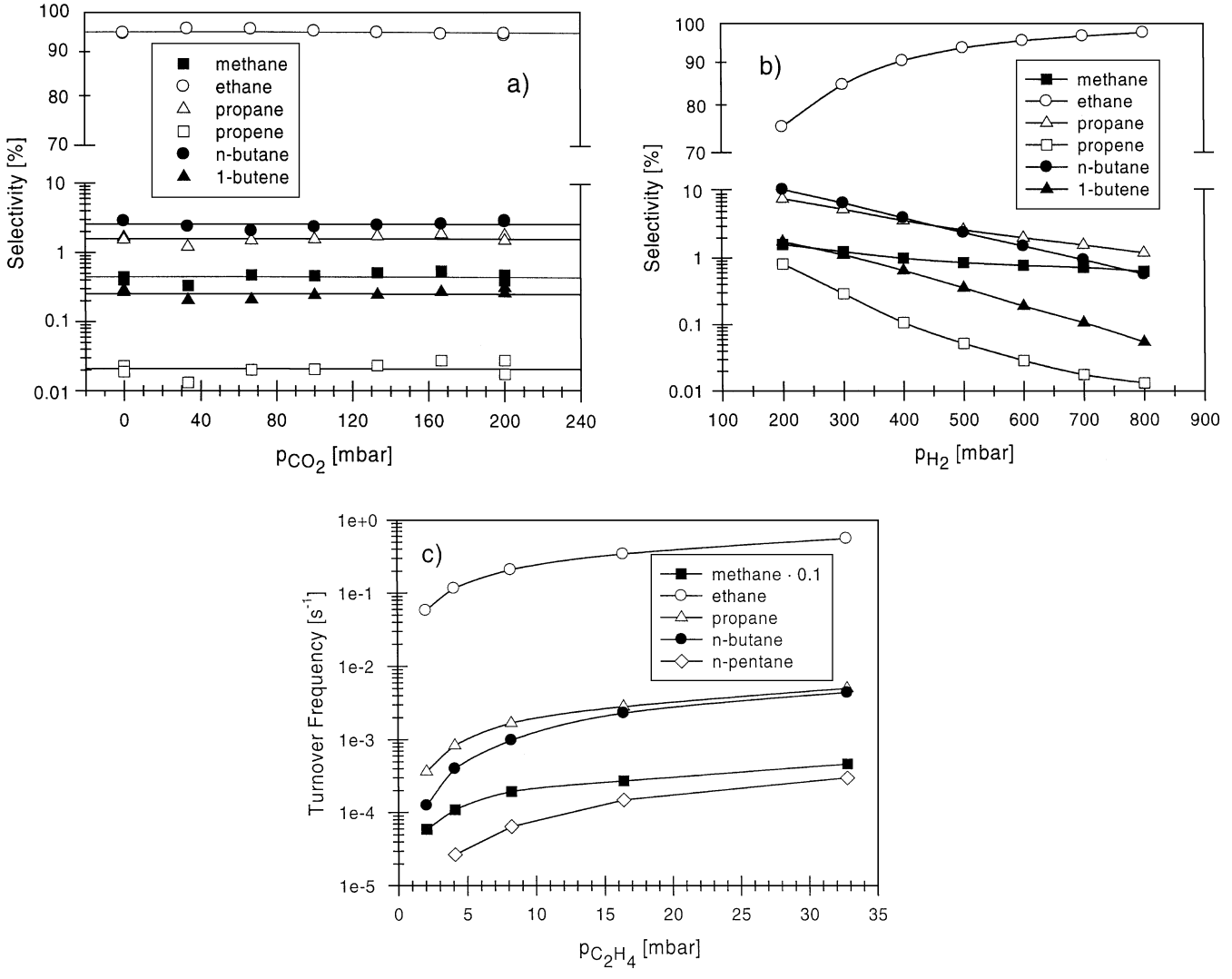

FIG. 2. (a) Selectivity of the hydrogenation of ethene as a function of the carbon dioxide pressure at $T = 433$ K. (b) Selectivity of the hydrogenation of ethene as a function of the hydrogen pressure at $T = 433$ K. (c) Turnover frequency of the product gases as a function of the partial pressure of ethene at $T = 433$ K.

This affects the formation of unsaturated hydrocarbons (propene and 1-butene) more than the formation of saturated hydrocarbons (propane and *n*-butane), since the unsaturated hydrocarbons are reactive intermediates, which are easily hydrogenated to the saturated compounds. In this way the sequence in the selectivity can be changed in dependence on the hydrogen pressure (see propane and butane). The formation of methane, i.e., the fragmentation reaction, is much less influenced by the hydrogen pressure.

3.1.3. Influence of the partial pressure of ethene on the turnover frequencies of the hydrogenation reactions. These experiments were also performed at $T = 433$ K. The partial pressures were $p(CO_2) = 200$ mbar, $p(H_2) = 800$ mbar, $p(C_2H_4) =$ variable. The volumetric feed rate was 60 ml_N/min.

In Fig. 2c the logarithm of the turnover frequency of the product gases has been plotted against the partial pressure of ethene. As expected the turnover frequencies increase with increasing ethene pressure, since under the given conditions the active sites are not saturated with ethene. The conversion of ethene amounts to >90%; i.e. the gas leaving the reactor still contains ethene. This situation will prove to be the cause for the observation that carbon dioxide is not at all hydrogenated in these experiments.

3.1.4. Influence of temperature on the selectivity of the hydrogenation reactions. The influence of the reaction temperature on the hydrogenation reactions has been compiled in Table 1 for the temperature range from 433 to 523 K. The composition of the feed was $p(H_2) = 800$ mbar, $p(CO_2) = 200$ mbar, $p(C_2H_4) = 16$ mbar, and the volumetric feed rate amounted to 60 ml_N/min.

The total selectivity of all the hydrocarbons not mentioned in Table 1 was less than 1%. At all temperatures the reactions which occur are dominated by the direct hydrogenation of ethene. However, the fragmentation of ethene strongly increases with temperature. This influences not only the formation of methane but also the formation of propane, *n*-butane, and *n*-pentane. The observation that the selectivity for the latter two products passes through a maximum is due to the increase of hydrogenolysis as will be discussed later on. The trends following from Table 1 are independent of the partial pressure of carbon dioxide. They are even valid in the absence of carbon dioxide.

TABLE 1

Influence of Temperature on the Selectivity of the Hydrogenation Reactions

Temperature (K)	Methane	Ethane	Propane	*n*-Butane	*n*-Pentane
433	1.0	94.5	2.3	1.2	0.1
463	4.6	85.3	5.8	3.2	0.3
493	11.5	75.8	8.0	3.4	0.6
523	27.7	63.1	6.3	2.0	0.3

3.2. Hydrogenation of Carbon Dioxide–Ethene Mixtures in a Batch Reactor

The situation changes when the catalytic reaction is not carried out in a plug-flow reactor under steady state conditions, but in a batch reactor, i.e., in a closed system. Then, according to the results dealt with in the preceding paragraph, after some time the store of ethene will be consumed and the hydrogenation of carbon dioxide will follow. Therefore studies by means of a batch reactor will be suitable to investigate the mutual influences of carbon dioxide and ethene in hydrogenation reactions in more detail.

3.2.1. The induction period. The reaction described in Fig. 3a was performed in the batch reactor at 523 K under the initial conditions $p(H_2) = 800$ mbar, $p(CO_2) = 200$ mbar, $p(C_2H_4) = 80$ mbar. In this case it is expedient to plot the concentrations of the substances in the gas phase as a function of reaction time. It is evident that there is a rather long induction period before the reactions start. This is due to the circumstance that the cleaning process of the cobalt foil ended with an oxidation step, i.e., that at the beginning the catalyst surface consists of cobalt oxide. Figure 3a shows that neither carbon dioxide nor ethene can be hydrogenated over the oxidised surface. Between 30 and 60 min the hydrogenation of ethene starts accompanied by fragmentation under the formation of methane. Only when most of the ethene has been consumed the hydrogenation of carbon dioxide sets in. At a reaction time of 90 min the conversion of ethene amounts to 89% and that of carbon dioxide to 1%. At 120 min nearly no ethene has been left. From this time onward no significant increase in the concentration of ethane can be observed. There is, however, a strong formation of methane, the main product with the hydrogenation of carbon dioxide. As soon as carbon dioxide begins to react carbon monoxide can be detected, however, only in a very small concentration.

The vertical dotted lines in Fig. 3a mark the reaction times at which the catalyst has been transferred via the differentially pumped lock system into the UHV chamber in order to take Auger electron spectra. For this time (about 15 min) the catalytic reaction is interrupted. As soon as the catalyst is brought back into the batch reactor the reaction goes on without any disturbance, as follows from the fact that the values of the concentrations determined before and after the interruption vary only within the limit of error.

Figure 3b shows the Auger electron spectra. Just at the beginning of the experiment the oxygen signal is dominating and the peak-to-peak height of the $L_3M_{45}M_{45}$ cobalt signal at 775 eV relative to the corresponding values of the $L_3M_{23}M_{23}$ and $L_3M_{23}M_{45}$ cobalt signals at 655 and 715 eV, respectively, indicate that the cobalt at the surface is not metallic.

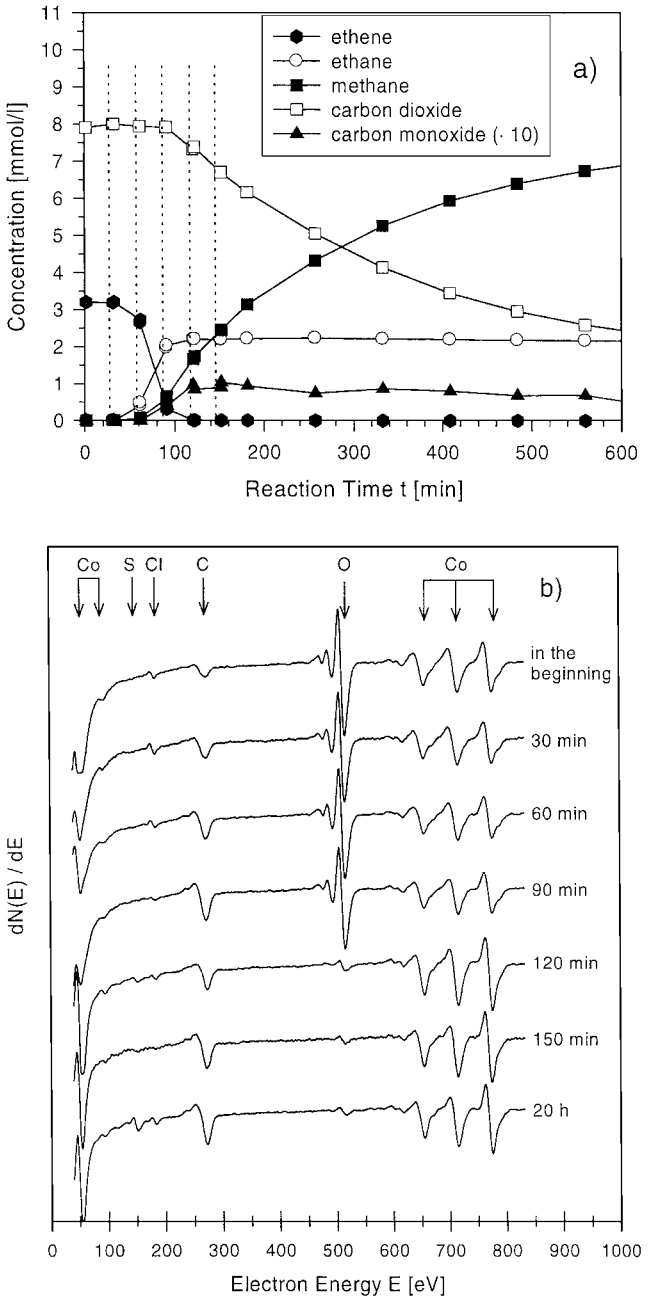

FIG. 3. (a) Hydrogenation of carbon dioxide and ethene on cobalt foils in a batch reactor at $T = 523$ K. The dashed lines represent where the Auger electron spectra of Fig. 3b were taken. (b) Auger electron spectra of the cobalt foil taken during the hydrogenation reaction.

The ratio of the peak-to-peak heights of the signals of oxygen and cobalt at 515 and 775 eV, respectively, remain nearly constant up to $t = 90$ min. Between 90 and 120 min this ratio diminishes by a factor of $6 \cdot 10^{-2}$. Simultaneously the cobalt signal at 775 eV increases relative to the cobalt signals at 655 and 716 eV. This observation clearly indicates that the reduction of the surface occurs mainly between 90 and 120 min, just when the ethene has been consumed.

The reduction of the oxidic surface needs atomic hydrogen which can only be formed on the metallic surface. The same holds for the hydrogenation of ethene which is also adsorbed only on the metallic surface. Hydrogen and ethene compete for the initially small number of metallic sites. In this way ethene hinders the reduction of the cobalt oxide. The same effect has been observed with carbon monoxide, which prolongs the induction period, when carbon dioxide is hydrogenated over initially oxidised cobalt (20).

When the cleaning procedure of the cobalt foil is not finished with the oxidation step but with reduction no induction period exists, the reaction between ethene, carbon dioxide, and hydrogen starts immediately with the hydrogenation of ethene. Already after 4 min 70% of the initial amount of ethene have been consumed. When after 30 min the second sample is taken for gas chromatographic analysis no ethene can be detected and already 20% of the initial amount of carbon dioxide have been hydrogenated. At a reaction time of 560 min the composition of the gas phase is identical with that shown in Fig. 3a for the same reaction time.

3.2.2. Byproducts formed during the induction period. The rather slow rate of reaction during the induction period allows a detailed analysis of the composition of the gas phase. In Fig. 4a the logarithms of the concentrations of the saturated hydrocarbons are plotted in dependence on the reaction time. The approximately constant slope of the curves between 30 and 90 min points to an approximately exponential increase of their concentrations with time. It is evident that the higher hydrocarbons are only formed as long as ethene is available. That means that they are not a product of the hydrogenation of carbon dioxide. The selectivities determined after a reaction time of 90 min are in the cases of CH_4 10.8%, C_2H_6 70.2%, C_3H_8 7.9%, C_4H_{10} 4.5%, and C_5H_{12} 0.6%.

Figure 4b shows that during the induction period also the corresponding unsaturated hydrocarbons are formed. However, as soon as the concentration of ethene has dropped to only some percent of its inital value they disappear completely. They seem to be active intermediates, which are replaced from the surface by ethene before they can be hydrogenated. However, when the ethene concentration is low enough, they are readsorbed and hydrogenated.

The correctness of this argumentation is supported by the fact that up to 200 min the carbon content of all hydrocarbons is balanced within an error of $\pm 2.5\%$ when carbon dioxide is not taken into account.

3.2.3. Hydrogenation of ethene in the batch reactor in absence of carbon dioxide. The results discussed in the preceding paragraphs seem not to show any influence of carbon dioxide on the reactions as long as ethene is present. In order to check whether this statement is correct, the hydrogenation of ethene in the batch reactor should also be

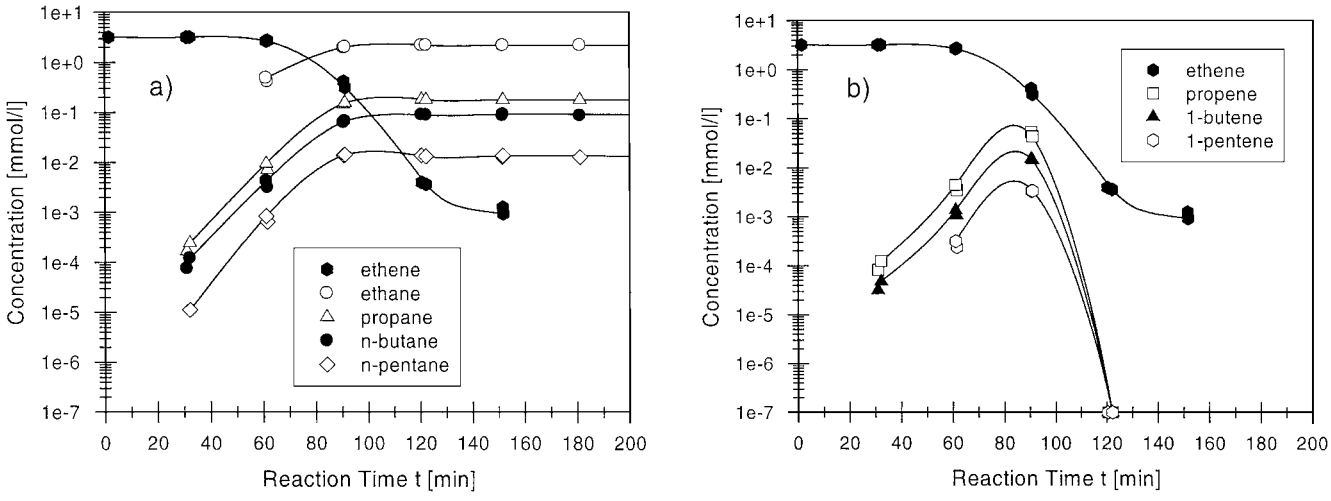

FIG. 4. (a) Concentration of the saturated hydrocarbons in dependence on the reaction time. (b) Concentration of the unsaturated hydrocarbons in dependence on the reaction time.

studied in the absence of carbon dioxide as was done in the case of the experiments with the plug-flow reactor (see Fig. 2a, $p(CO_2) = 0$ mbar). For this purpose carbon dioxide was substituted by neon. The initial composition of the gas phase was $p(H_2) = 800$ mbar, $p(Ne) = 200$ mbar, $p(C_2H_4) = 80$ mbar; the reaction temperature was $T = 523$ K. The catalyst cleaning was finished with the oxidation step.

In Fig. 5a the concentrations of ethene, ethane, and methane have been plotted in dependence on the reaction time. The induction period is considerably shorter than in the presence of carbon dioxide (Fig. 3a). It is more pronounced for the fragmentation reaction than for the hydrogenation of ethene. The fact that carbon dioxide prolongs the induction period without being involved in the hydrogenation reactions points most likely to the formation of a carbonate species on the oxidised cobalt surface, which is responsible for the long induction period. The formation of carbonate after coadsorption of oxygen and carbon dioxide on transition metal surfaces (24, 25) or after adsorption of carbon dioxide on metal oxide surfaces (26) is well known from the literature.

Already after 60 min ethene has disappeared from the gas phase. The following changes in the concentrations of the products have to be traced back to consecutive reactions. As can be seen from Fig. 5b the product spectrum just after the consumption of ethene is very similar to that observed in Figs. 3a, 4a, and 4b, when carbon dioxide had not yet begun to react. The concentrations of all products with the exception of methane pass through a maximum at 90 min. Then they decrease, whereas the methane concentration still increases. That means that hydrogenolysis under formation of the thermodynamically more stable methane takes place. Since all curves in Fig. 5b (logarithm of concentration against time) are straight lines this hydrogenolysis occurs in first order kinetics (27). The rate constants have been compiled in Table 2. The rate constant of hydrogenolysis increases with increasing chain length; linear hydrocarbons react faster than branched hydrocarbons.

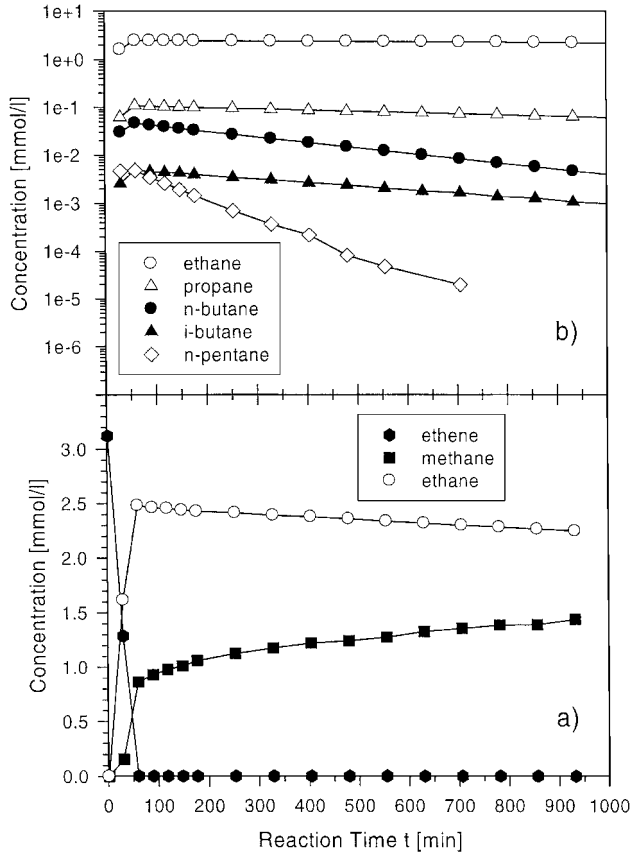

FIG. 5. Hydrogenation of ethene in the absence of carbon dioxide on cobalt foils in a batch reactor at $T = 523$ K.

TABLE 2

Rate Constants of Hydrogenolysis at 523 K

Hydrocarbons	k_1 (min^{-1})
Ethane	$5.35 \cdot 10^{-5}$
Propane	$2.53 \cdot 10^{-4}$
n-Butane	$1.10 \cdot 10^{-3}$
i-Butane	$7.26 \cdot 10^{-4}$
n-Pentane	$4.17 \cdot 10^{-3}$
Ethene	$1.10 \cdot 10^{-2}$

Hydrogenolysis cannot be observed in the presence of carbon dioxide, i.e., when mixtures of carbon dioxide and ethene or pure carbon dioxide are hydrogenated. When carbon dioxide (or carbon monoxide) had been completely hydrogenated and the water vapour had been removed by freezing out in a cooling trap, hydrogenolysis of ethane and propane was observed (19). The rate constants agreed with those given in Table 2. This observation can be explained by the assumption that carbon monoxide, carbon dioxide, and water compete with the hydrocarbons for adsorption sites and are more strongly bonded to the surface than the latter ones.

3.3. Mechanism of the Formation of Higher Hydrocarbons in Ethene–Hydrogen–Carbon Dioxide Mixtures over Cobalt

As shown in Fig. 2a carbon dioxide does not at all influence the selectivity of the hydrogenation reactions, in contrast to the behaviour of hydrogen (Fig. 2b). An increase of the partial pressure of hydrogen leads even to a change in the sequence of the formed hydrocarbons in the selectivity scale. From the data of Fig. 2b the mole fraction of the hydrocarbons can be calculated in dependence on the number *n* of carbon atoms. This has been done in Fig. 6 for partial pressures of hydrogen of 200 and 800 mbar, respectively. The partial pressure of ethene was in both cases 16 mbar. As already mentioned the formation of the hydrocarbons with an even number of C atoms is favoured before the formation of the molecules with an odd number of C atoms. This partially leads to an oscillating behaviour of the curves in Fig. 6.

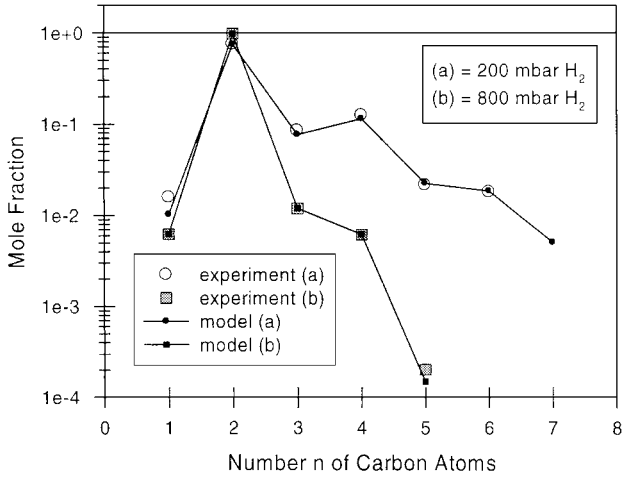

FIG. 6. Mole fraction of the hydrocarbons calculated from the data of Fig. 2b in dependence on the number, *n*, of carbon atoms.

In the following an attempt is made to describe the mechanism of the chain growth quantitatively. It is based on an approach made by Novak *et al*. (28) and successfully applied by Jordan *et al*. (29) in order to explain oscillations in the weight distribution for chain growth in Fischer–Tropsch synthesis.

In the preceding paragraphs it has been discussed that besides hydrogenation of ethene and chain growth, fragmentation of ethene also takes place. This means that chain growth could occur by both C_1 and independent C_2 addition. This situation is explained in Fig. 7a. It refers to the steady-state conditions in the plug-flow reactor.

The rate of desorption of the hydrocarbon with *n* carbon atoms ($C_{n,g}$) into the gas phase is given by the product $k_t\Theta_n$ where Θ_n is the fraction of active sites occupied by the adsorbate C_n and k_t is the rate constant of desorption, i.e., the rate constant of the termination reaction. The rate of formation of C_n in the adsorbed layer is given on one hand by the surface concentration of C_{n-1} (Θ_{n-1}), the surface concentration of C_1 (Θ_1), and the rate constant of this propagation reaction ($k_{p,1}$), i.e. by $k_{p,1}\Theta_{n-1}\Theta_1$ and on the other hand by the surface concentration of C_{n-2} (Θ_{n-2}), the surface concentration of C_2 (Θ_2), and the rate constant of the corresponding propagation reaction ($k_{p,2}$), i.e., by $k_{p,2}\Theta_{n-2}\Theta_2$. Θ_n decreases not only by desorption of C_n but also by the propagation reactions forming C_{n+1} and C_{n+2}, respectively. The corresponding reaction rates are $k_{p,1}\Theta_1\Theta_n$ and $k_{p,2}\Theta_2\Theta_n$, respectively. Under steady-state conditions Θ_n does not change with time, i.e.,

$$\Theta_n = 0 = k_{p,1}\Theta_1\Theta_{n-1} + k_{p,2}\Theta_2\Theta_{n-2} - k_t\Theta_n - k_{p,1}\Theta_1\Theta_n - k_{p,2}\Theta_2\Theta_n. \quad [1]$$

Since also Θ_1 and Θ_2 do not change under steady-state conditions Eq. [1] can be simplified by introducing

$$k'_{p,1} = k_{p,1}\Theta_1 \quad \text{and} \quad k'_{p,2} = k_{p,2}\Theta_2 \quad [2]$$

resulting in

$$\Theta_n = 0 = k'_{p,1}\Theta_{n-1} + k'_{p,2}\Theta_{n-2} - k_t\Theta_n - k'_{p,1}\Theta_n - k'_{p,2}\Theta_n \quad [3]$$

or

$$\Theta_n = \frac{k'_{p,1}}{k_t + k'_{p,1} + k'_{p,2}}\Theta_{n-1} + \frac{k'_{p,2}}{k_t + k'_{p,1} + k'_{p,2}}\Theta_{n-2}. \quad [4]$$

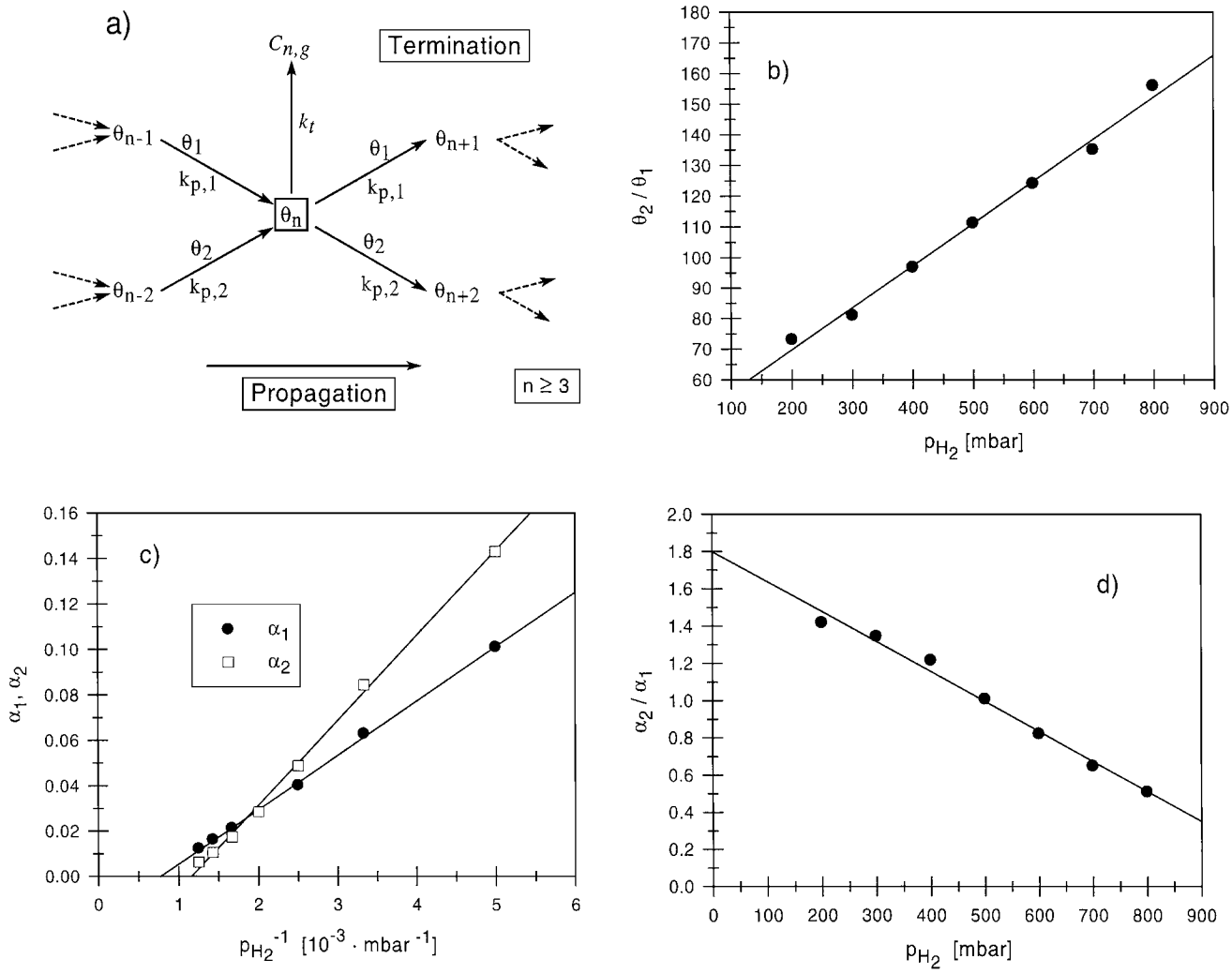

FIG. 7. (a) Reaction model of the hydrogenation of ethene at cobalt surfaces. See text for further explanations. (b) Θ_2/Θ_1 as a function of the hydrogen pressure at $T = 433$ K and an ethene pressure of 16 mbar. (c) Probabilities of chain growth α_1 and α_2 in dependence on the reciprocal of the hydrogen pressure. (d) Ratio α_2/α_1 in dependence on the hydrogen pressure.

When

$$\alpha_1 = \frac{k'_{p,1}}{k_t + k'_{p,1} + k'_{p,2}} \quad \text{and} \quad \alpha_2 = \frac{k'_{p,2}}{k_t + k'_{p,1} + k'_{p,2}} \qquad [5]$$

are introduced Eq. [4] can be written as

$$\Theta_n = \alpha_1 \Theta_{n-1} + \alpha_2 \Theta_{n-2}. \qquad [6]$$

α_1 and α_2 represent the probabilities of chain growth by C_1 and C_2 species, respectively. In order to be able to calculate the mole fraction

$$\frac{\Theta_n}{\sum_{n=1}^{\infty} \Theta_n} = \frac{\alpha_1 \Theta_{n-1} + \alpha_2 \Theta_{n-2}}{\sum_{n=1}^{\infty} (\alpha_1 \Theta_{n-1} + \alpha_2 \Theta_{n-2})} \qquad [7]$$

Θ_n has to be expressed as a function of n. A solution of the form

$$\Theta_n = x^{n-1} \qquad [8]$$

is tried by Novak *et al.* (28). Under these conditions Eq. [6] is given by

$$x^{n-1} = \alpha_1 x^{n-2} + \alpha_2 x^{n-3} \qquad [9]$$

which is equivalent to

$$x^2 - \alpha_1 x - \alpha_2 = 0. \qquad [10]$$

The solution of this equation is

$$x_{1,2} = \frac{1}{2}\left(\alpha_1 \pm \sqrt{\alpha_1^2 + 4\alpha_2}\right). \qquad [11]$$

The general solution of Eq. [6] is therefore

$$\Theta_n = Ax_1^{n-1} + Bx_2^{n-1}. \quad [12]$$

The coefficients A and B can be determined by the boundary conditions for $n=1$ and $n=2$, respectively. It follows that

$$A = \frac{\Theta_2 - \Theta_1 x_2}{x_1 - x_2} \quad \text{and} \quad B = \frac{\Theta_1 x_1 - \Theta_2}{x_1 - x_2} \quad [13]$$

and

$$\Theta_n = \frac{\Theta_2 - \Theta_1 x_2}{x_1 - x_2} x_1^{n-1} + \frac{\Theta_1 x_1 - \Theta_2}{x_1 - x_2} x_2^{n-1}. \quad [14]$$

The mole fraction is given by

$$\frac{\Theta_n}{\sum_{n=1}^{\infty} \Theta_n} = \frac{Ax_1^{n-1} + Bx_2^{n-1}}{\sum_{n=1}^{\infty} \left(Ax_1^{n-1} + Bx_2^{n-1}\right)}. \quad [15]$$

$$\sum_{n=1}^{\infty} Ax_1^{n-1} = A\left(x_1^0 + x_1^1 + x_1^2 + \cdots\right) = \frac{1}{1-x_1}, \quad [16]$$

since $x_1 < 1$, as follows from Eq. [11]. Inserting Eq. [16] into Eq. [15] leads to

$$\frac{\Theta_n}{\sum_{n=1}^{\infty} \Theta_n} = \frac{Ax_1^{n-1} + Bx_2^{n-1}}{\frac{A}{1-x_1} + \frac{B}{1-x_2}}. \quad [17]$$

This equation was used to fit the experimental data plotted in Fig. 6. In order to reduce the fit parameters from four (α_1, α_2, Θ_1, Θ_2) to three (α_1, α_2, r) the coverages Θ_1 and Θ_2 were substituted by the ratio of the coverages

$$r = \frac{\Theta_2}{\Theta_1}, \quad [18]$$

so that A and B are finally given by

$$A = \frac{\Theta_1(r - x_2)}{x_1 - x_2} \quad \text{and} \quad B = \frac{\Theta_1(x_1 - r)}{x_1 - x_2}. \quad [13a]$$

When A and B are defined in this way (Eq. [13a]) Θ_1 no longer appears in the mole fraction.

The values of the mole fraction in dependence on n determined on the basis of Eq. [17] by means of a least-square-fit have been plotted in Fig. 6 as small symbols. The result is astonishingly good, not only in the case of partial pressures of hydrogen of 200 and 800 mbar, but also for the whole range between these limiting pressure values. The fit procedures deliver the corresponding values of Θ_2/Θ_1, α_1, and α_2 in dependence on p_{H_2} and $p_{C_2H_4}$, respectively.

Figure 7b shows that there is a linear relationship between Θ_2/Θ_1 and p_{H_2} over the whole range of applied hydrogen pressures. The partial pressure of ethene amounted to 16 mbar and the temperature was 433 K. Θ_2, the coverage of C_2 intermediates, exceeds that of C_1 intermediates (Θ_1) by about two orders of magnitude. This corresponds rather well with the selectivities of the formation of ethane and methane, respectively. The increase of Θ_2/Θ_1 with increasing p_{H_2} may be due to an increase of Θ_2, to a decrease of Θ_1, or to a superposition of both effects. Most likely the direct hydrogenation of ethene is favoured with increasing hydrogen pressure with the consequence that the fragmentation reaction falls off. The same holds for the formation of the higher hydrocarbons, and it is not surprising that the unsaturated hydrocarbons are even more effected than the saturated ones.

The probabilities of chain growth, α_1 and α_2, exhibit a linear relationship to the reciprocal of the hydrogen pressure (Fig. 7c), at least in the range of the applied hydrogen pressures. This becomes easy to understand, when Eqs. [5] are taken into account. In the same way as $k'_{p,1} = k_{p,1}\Theta_1$ (Eq. [2]) k_t comprises the coverage of hydrogen or the hydrogen pressure, respectively. Both Θ_H and p_{H_2} are constants under steady-state conditions. Independent of whether the hydrogenation of the chemisorbed, probably di-σ-bonded species occurs via a Langmuir–Hinshelwood or an Eley–Rideal mechanism immediately followed by desorption k_t comprises p_{H_2}. When $k_t \gg k'_{p,1}$, $k_{p,2}$, the denominator in Eq. [5] is dominated by k_t, which is probably the case since α_1 and α_2 are in the order of magnitude of 10^{-2} to 10^{-1}, i.e., α_1 and α_2 are proportional to the reciprocal of p_{H_2}.

The ratio α_2/α_1, which does not contain k_t, is on the order of magnitude of 1 and decreases linearly with p_{H_2} (Fig. 7d), as far as 200 mbar $< p_{H_2} <$ 800 mbar. Since

$$\frac{\alpha_2}{\alpha_1} = \frac{k'_{p,2}}{k'_{p,1}} = \frac{k_{p,2}\Theta_2}{k_{p,1}\Theta_1} \quad [19]$$

the ratio of the rate constants $k_{p,2}$ and $k_{p,1}$ can be calculated, because the ratio Θ_2/Θ_1 is known. The ratio $k_{p,2}/k_{p,1}$ varies from 0.02 ($p_{H_2} = 200$ mbar) to 0.003 ($p_{H_2} = 800$ mbar), i.e., the rate constant $k_{p,2}$ of the chain growth via C_2 is by 2 to 3 orders of magnitude smaller than the rate constant $k_{p,1}$ of chain growth via C_1.

This section was so named because the results were obtained with such gas mixtures. However, it has been clearly demonstrated in the other paragraphs that under the given conditions CO_2 does not at all influence the reactions taking place. Therefore the discussed findings are characteristic of the chain growth accompanying the hydrogenation of ethene over Co and should not be compared with similar observations made with Fischer–Tropsch reactions.

4. CONCLUSIONS

The experiments carried out with the plug-flow reactor clearly show that the hydrogenation of carbon dioxide is blocked as long as ethene is present in the gas phase. On the other hand the presence of carbon dioxide does not at all influence the hydrogenation of ethene. An increase in the hydrogen pressure favours the hydrogenation of ethene to ethane and detracts greatly from the chain growth. An increase of the partial pressure of ethene leads to a pronounced chain growth. The formation of methane (also in the absence of carbon dioxide) proves that fragmentation of ethene takes place. This observation is contrary to the statements of Adesina *et al*. (21).

The use of the batch reactor allowed the correlation of the gas phase measurements with the state of the catalyst observed by means of Auger electron spectroscopy. When the experiment is started with the oxidised catalyst an induction period is observed in the course of which the catalyst is reduced. During this period the hydrogenation of carbon dioxide is totally blocked, whereas ethene begins to be hydrogenated. The oxygen signal in the Auger electron spectrum disappears when nearly all the ethene has been hydrogenated. Only then does carbon dioxide hydrogenation start. It is interesting to note that the presence of carbon dioxide prolongs the induction period, possibly by the formation of carbonate. The hydrogenation of pure ethene in the batch reactor allows us to recognise that the olefines are formed as intermediates and that at long reaction times hydrogenolysis of the saturated hydrocarbons takes place.

The oscillatory behaviour of the molar fraction of the products in dependence on the number of C atoms, which was observed with the hydrogenation of ethene, could quantitatively be interpreted by a chain growth mechanism regarding chain growth by incorporation of both C_1 and C_2 species.

ACKNOWLEDGMENTS

This work was financially supported by the Fonds der Chemischen Industrie and the Max-Buchner-Forschungsstiftung.

REFERENCES

1. Storch, H. H., *Adv. Catal.* **1**, 115 (1948).
2. Pichler, H., *Adv. Catal.* **4**, 271 (1952).
3. Pichler, H., and Schulz, H., *Chem.-Ing.-Tech.* **42**, 1162 (1970).
4. Biloen, P., and Sachtler, W. M. H., *Adv. Catal.* **30**, 165 (1981).
5. Schulz, H., Beck, K., and Erich, E., *in* "Proc. Methane Conv. Symposium, Auckland 1987" (D. Bibby, C. Chang, R. Howe, and S. Yurchak, Eds.), *Stud. Surf. Sci. Catal.* **36**, 457 (1988).
6. Adesina, A. A., *Appl. Catal. A* **138**, 345 (1996).
7. Kuipers, E. W., Vinkenburg, I. H., and Oosterbeek, H., *J. Catal.* **152**, 137 (1995).
8. Kuipers, E. W., Scheper, C., Wilson, J. H., Vinkenburg, I. H., and Oosterbeek, H., *J. Catal.* **158**, 288 (1996).
9. Lee, W. H., and Bartholomew, C. H., *J. Catal.* **120**, 256 (1989).
10. Voß, M., Thesis, University of Erlangen-Nürnberg, 1998. (Publication in preparation.)
11. Weatherbee, G. D., and Bartholomew, C. H., *J. Catal.* **87**, 352 (1984).
12. Sexton, B. A., and Somorjai, G. A., *J. Catal.* **46**, 167 (1977).
13. Solymosi, F., and Erdöhelyi, A., *J. Mol. Catal.* **8**, 471 (1980).
14. Solymosi, F., Erdöhelyi, A., and Bánsági, T., *J. Catal.* **68**, 371 (1981).
15. Iglesia, E., Soled, S. L., and Fiato, R. A., *J. Catal.* **137**, 212 (1992).
16. Weatherbee, G. D., and Bartholomew, C. H., *J. Catal.* **7**, 460 (1982).
17. Wetzel, H., Meyer, G., Borgmann, D., and Wedler, G., *Chem.-Ing.-Tech.* **63**, 613 (1991).
18. Fröhlich, G., Kestel, U., Łojewska, J., Łojewski, T., Meyer, G., Voß, M., Borgmann, D., Dziembaj, R., and Wedler, G., *Appl. Catal. A: Gen.* **134**, 1 (1996).
19. Fröhlich, G., Thesis, University of Erlangen-Nürnberg, 1996. (Publication in preparation.)
20. Kestel, U., Fröhlich, G., Borgmann, D., and Wedler, G., *Chem. Eng. Technol.* **17**, 390 (1994).
21. Adesina, A. A., Hudgins, R. R., and Silveston, P. L., *Appl. Catal.* **62**, 295 (1990).
22. Percy, L. T., and Walter, R. I., *J. Catal.* **121**, 228 (1990).
23. Borgmann, D., Strattner, P., and Wedler, G., *Chem.-Ing.-Tech.* **58**, 400 (1986).
24. Pirner, M., Borgmann, D., and Wedler, G., *Surf. Sci.* **211/212**, 1091 (1989).
25. Wedler, G., Kießling, W., and Borgmann, D., *Vacuum* **41**, 93 (1990).
26. Freund, H.-J., and Roberts, M. W., *Surf. Sci. Rep.* **25**, 225 (1996).
27. Boudart, M., and Djéga-Mariadassou, G., "Kinetics of Heterogeneous Catalytic Reactions." Princeton University Press, Princeton, 1984. (Further references therein.)
28. Novak, S., Madon, R. J., and Suhl, H., *J. Chem. Phys.* **74**, 6083 (1981).
29. Jordan, D. S., and Bell, A. T., *J. Phys. Chem.* **90**, 4797 (1986).